Future wing Hybrid Laminar Flow Control suction system design and analysis

Dr James Alderman
Airbus Group Innovations, BS34 7QW, United Kingdom, James.Alderman@eads.com

Dr Michael Meyer
Airbus Group Innovations, 81663, Germany, Michael.X.Meyer@airbus.com

Mikael Bottemanne
Airbus Group Innovations, 81663, Germany, Mikael.Bottemanne@airbus.com

Prof Chris Atkin
City University London, EC1V 0HB, United Kingdom, Chris.Atkin.1@city.ac.uk

Alan Mann
Airbus Operations Ltd, BS99 7AR, United Kingdom, Alan.Mann@airbus.com

ABSTRACT

The work presented is part of the Active wing active Flow - Loads & Noise control on next generation wing (AFLoNext) project work package 1.2 which aims to prove the engineering feasibility of the Hybrid Laminar Flow Control (HLFC) technology for drag reduction on a wing by means of large scale ground-based demonstrator. This paper describes the design of an aerofoil pressure distribution philosophy and self adapting suction distribution while obeying constraints imposed by a particular suction skin concept and ice protection system. Models were developed to make assessment of the HLFC system pressure losses allowing the definition of suction distributions that maximise the benefits of HLFC by balancing increased laminarity with pump drag and mass increases. Finally, sensitivity studies are undertaken to understand drag implications of spanwise suction variations.

1 INTRODUCTION

A focus for the continued development of civil transport aircraft is the reduction of fuel burn and carbon emissions. The airframer can directly influence this by reducing airframe drag. Two ways of achieving this is to increase the wing span (reduction in vortex drag) or as is the subject of this paper to reduce the viscous drag by achieving laminar flow on a portion the wing windswept surfaces.

As the cruise Mach number increases beyond Mach 0.70 it becomes increasingly difficult for wing shape alone to maintain a laminar boundary layer due to the increased Reynolds number and sweep effects. The use of Hybrid Laminar Flow Control (HLFC) can potentially alleviate this situation by applying suction ahead of the wing box, flow is ingested through the wind-swept surface stabilising the laminar boundary layer and delaying boundary layer transition.

Applying HLFC to the wing leading edge is not a simple undertaking since many systems need to be integrated into the leading edge namely; load carrying structure, suction skin, high lift / shielding device, ice protection system and HLFC suction system.

This paper builds on the knowledge of the HYLTEC project developing models for the pressure loss associated with HLFC suction systems and developing a methodology for creating self adapting suction distributions over a range of flight conditions.

The use case studied in this paper is based on the outer wing of a future long range aircraft with the following characteristics: Mach=0.82, Altitude=33,000ft, Λ_{LE}=32.0°, Λ_{TE}=19.8°, Chord=3.489m, C_l = 0.48, 0.55, 0.63.

2 DESIGN AND ANALYSIS TOOLSET

This section describes the toolset used for the design and analysis of an aerofoil, suction distribution and characteristics of the HLFC system within AFloNext WP1.2. This work package described a use case based on the outer wing of a future long range aircraft. Due to the large number of design iterations expected the decision was made to use a relatively fast running toolset. The implication of this decision means that we limit the applicability of the analysis to spanwise suction chambers and the effects of spanwise chamber interruptions cannot be assessed.

2.1 Calculation of aerofoil characteristics (base flow)

The flow characteristics of the outer wing can be approximated with 2D transonic aerofoil methods using the appropriate Lock transformations for sweep & taper[1]. The tool chosen for this is the CVGK[2,3] transonic aerofoil solver which itself is derived from the BVGK[4] aerofoil code that is widely used within the UK aerospace industry. CVGK differs from BVGK in two major ways with the Airbus UK Callisto[5] method used for the viscous calculations and the inclusion of corrections on the base flow to account for the effects of sweep and taper[1].

2.2 Boundary layer stability analysis

In order to make assessment of a HLFC system, there is a requirement to calculate the extent of laminarity in response to changing flow conditions (C_l) and suction mass flow / distribution. The effects of suction on the development of a laminar boundary layer is calculated with the compressible boundary layer solver BL2D[6], and the extent of laminarity is computed with the classical linear e^N CoDS[7] solver. Within the AFloNext project critical N-factors for both Tollmien-Schlichting (TS) and Cross Flow (CF) were defined as NTS = 9 and NCF = 7. An additional N-factor constraint is applied to ensure CF N-factors are limited to NCF=5 at x/c<0.2.

2.3 Suction system characteristics

Previous EU research projects like HYLTEC[8] have developed suction pump performance and pump drag calculation methods while assuming a 99% pressure recovery of the HLFC ducting. Within AFloNext WP1.2, the HYLTEC work is refined by creating pressure loss models of the HLFC ducting which is crucial for assessment of the required suction pressure ratio of the suction system. Furthermore, the overall system mass including the suction pump and auxiliary infrastructure (pipe work valves) are calculated. This information is relevant to develop an optimal integrated technology solution.

Figure 1 presents an overview of the components of a typical HLFC suction system investigated within AFloNext WP1.2. The "Trunk duct" (1) transports the ingested boundary layer flow to a suction pump or region of low pressure to drive the HLFC suction system (this paper only considers a suction pump). "Collector ducts" (2) distributes the suction from the trunk duct to the "Spanwise Chambers" (3) via metering holes, that distribute the suction across the span allowing a proportion on the boundary layer to be ingested through the "Porous skin" (4). The sizing and number of the spanwise chambers, collector ducts, metering holes and the trunk duct diameter are free variables that are iterated to achieve a satisfactory compromise between aerodynamics and structures.

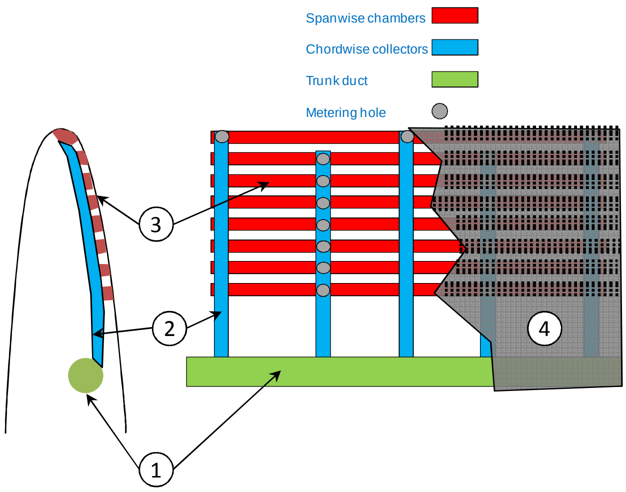

Figure 1: Typical HLFC suction system architecture investigated within AFloNext WP1.2

Pressure losses in pipes such as the spanwise chambers, chord wise collectors and trunk duct are generally expressed by

$$\Delta p = f \frac{L}{D} \rho \frac{u^2}{2} \qquad \textit{Equation 1}$$

where: f is the friction coefficient, L is the pipe length, D is the diameter of the pipe, ρ is the air density and u is the mean air flow velocity in the pipe. For determining f we use an approximation of the Colebrook White equation[9]:

$$f = 0.25 \Big/ \left[log\left(\frac{k}{3.7D} + \frac{5{,}74}{Re^{0.7}}\right)\right]^2$$ *Equation 2*

The variable k is the roughness of the pipe surface and Re is the Reynolds number based on the hydraulic diameter D. Corrections of non-circular cross sections use appropriate correction factors for laminar and turbulent flow states[10]. For the pipe flows further models are applied for merging/dividing flows, flows over porous surfaces, turning flows, flows through valves and orifice flows. The latter is especially relevant with respect to determining the correct metering hole diameters. Finding a metering hole design that is self-adapting and thus suitable for a bandwidth of flight conditions is challenging but feasible.

The mass flow pressure loss relationship and over suction criteria of porous panels are taken from HYLTEC experience and documented in HYLTEC TR-22 and TR-23 [11,12], these include upper limits of the suction hole Reynolds and Mach number. Within the AFloNext project these relationships are being investigated further to assess their validity. Additionally, a suction outflow constraint is applied whereby the suction chamber pressure is always 500Pa less than the external flow to ensure the chamber is always sucking so as not to cause bypass transition.

2.4 Calculation of performance metric

When defining a suction distribution for a HLFC equipped wing, it is useful to define a performance metric with which to compare design iterations. The performance metric chosen within AFloNext WP1.2 is a weighted sectional drag cost function defined in the following way:

$$CD_{cost} = CD_{net\_1} * f_1 + CD_{net\_2} * f_2 + ... + CD_{net\_n} * f_n$$ *Equation 3*

$$CD_{net\_n} = CD_v + CD_{pump} + CD_{mass}$$ *Equation 4*

Where:
n = index for design points
CD_v = Sectional viscous drag
CD_{pump} = Sectional drag increment attributed to suction pump power consumption
CD_{mass} = Sectional drag increment attributed to HLFC system mass
f_n = weighting factor

note: In this analysis wave drag is omitted since it is assumed that the aerofoil pressure distribution does not change with suction. The base flow pressure distribution is calculated with a representative transition location.

2.5 Suction optimisation framework

The previous sections have described the methods by which the characteristics of an aerofoil with a suction distribution may be calculated including the effects of the HLFC suction system, pump power requirements while ensuring the suction distributions are self adapting and may be achieved with a constant metering hole dimensions for a range of design points. It is clear that a large number of free variables can be used to define a HLFC aerofoil and these include:

- Aerofoil section shape *(constraints on spar location, t/c and aerofoil t/c_{max})*
- HLFC system architecture, number and size of HLFC ducting, skin porosity *(constrained by manufacturability, space allocation)*
- Position of suction chambers *(constrained with WIPS requirements)*
- Chamber Suction flow rates / chamber pressures *(constrained by suction criteria)*

One solution to this multi-dimensional problem would be to expose every variable to an optimisation algorithm and wait for an acceptable answer to emerge. This was not the approach taken within AFloNext WP1.2 but rather to use an optimisation algorithm to calculate chamber pressures that gave minimum CD_{net} for a given HLFC suction architecture and chamber locations shown Figure 2.

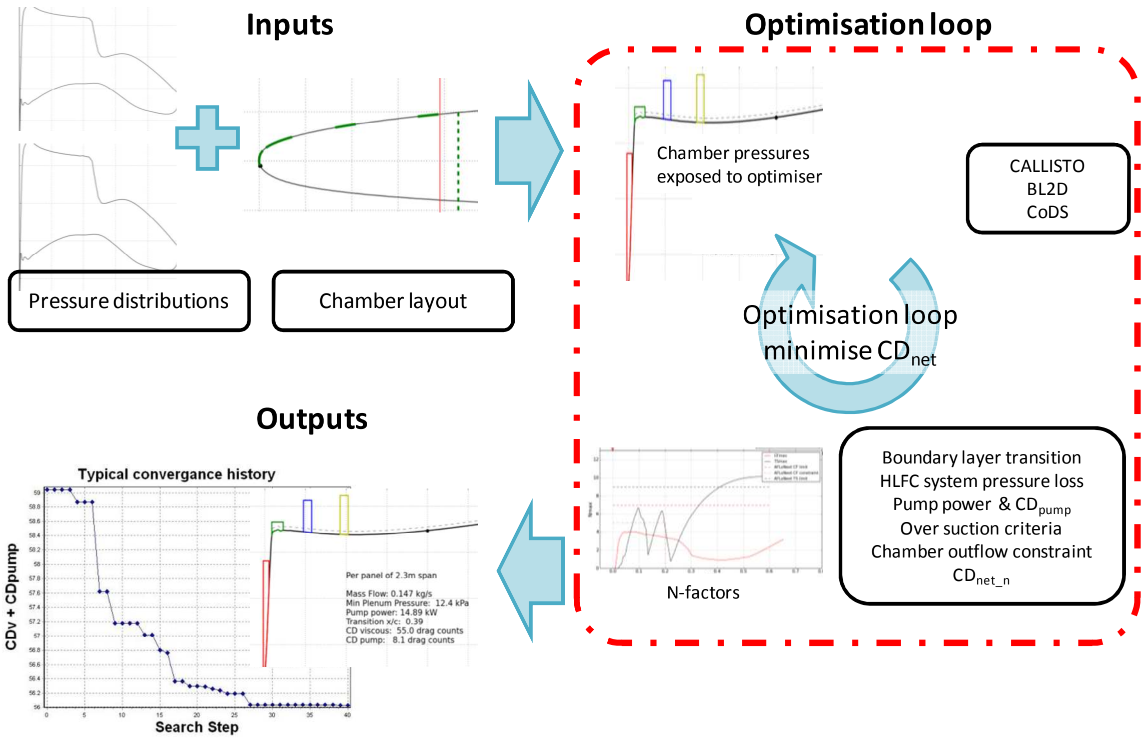

Figure 2: Diagram of chamber pressure optimisation process.

3 HLFC AEROFOIL DESIGN

This section describes the analysis undertaken to develop an aerofoil pressure distribution philosophy suitable for HLFC application described in[13]. The aim of this work was to define an aerofoil that meets the following requirements.

1. Minimum CD_{cost}
2. Maximise leading edge volume ahead of front spar
3. Increase leading edge radius to help high lift performance
4. Constant t/c_{max} and spar depths maintained or bettered than baseline aerofoil.

In order to investigate this, a family of aerofoils were designed with the roof top pressure gradients reducing from strongly accelerating to mildly decelerating. Figure 3 shows the pressure distributions of this family of aerofoils for the primary design point C_l=0.55, where there is a clear and expected trend of reduced wave drag as the roof top pressure gradient becomes less favourable. The effect of moving towards a less favourable roof top gradient is to increase leading edge volume.

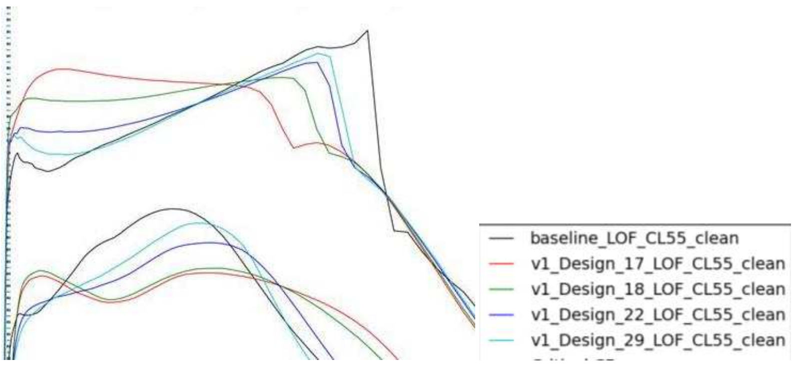

Figure 3: C_L=0.55 pressure distributions with roof top pressure gradient variation.

Figure 4 continues to show the sectional drag build up of the aerofoil family with a nominal suction chamber layout, but with the suction rates "optimised" for minimum CD_{net}. It is clear to see that Design_22 gives the lowest CDnet with the best compromise of CDv, CDw & CDpump. Further increases in CD_{net} are observed with increased leading edge volume since this increases the pump power requirement more than the wave drag is reduced due to adverse roof top pressure gradient associated with Design_17. It is worth indicating that CDv is increased since the more forward shock location of Design_17 limits the extent of laminarity.

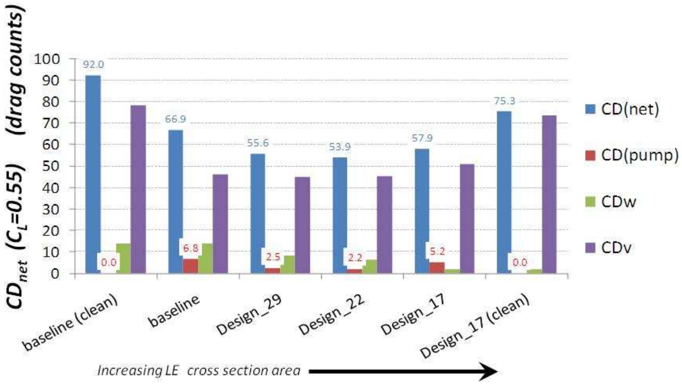

Figure 4: Sectional drag build up of aerofoil family with suction (C_l=0.55) (clean means no suction)

Figure 5 presents a comparison between the baseline aerofoil and the Design_22 aerofoil that was selected for use on the ground based demonstrator. It is clear to see that the Design_22 aerofoil has increased volume ahead of the front spar (3.6%) and increased leading edge radius that should help with integrating the components in the leading edge and improving high lift performance.

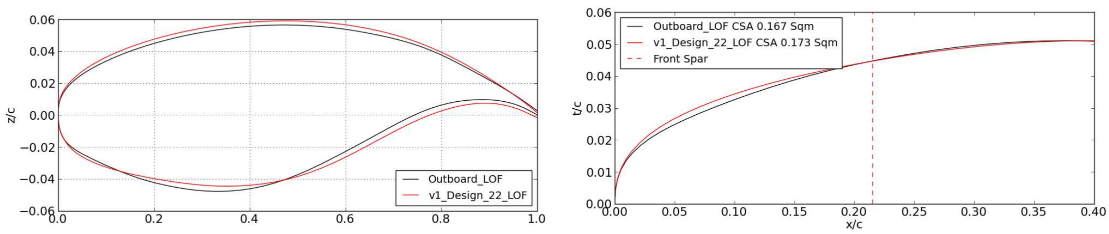

Figure 5: Comparison of Baseline aerofoil (black) with Design_22 (red)

4 STEPS TOWARDS OPTIMAL SUCTION DISTRIBUTIONS

This section will present some of the steps towards developing a spanwise chamber distribution that allows laminarity to be preserved while satisfying the constraints imposed by manufacturability and Wing Ice Protection System (WIPS) requirements. The suction skin concept selected for the ground based demonstrator within AFloNext WP1.2 is based on a SONACA patent[15], and a prototype part is shown in Figure 6. This part is produced with three sheets of titanium diffusion-bonded in specific locations, the internal spanwise chambers are formed when the part is inflated using SuperPlastic forming techniques. An interesting feature of this design concept is that it requires the use of hot bleed air from the turbofan compressor for the WIPS.

Figure 6: SONACA HLFC skin concept prototype from HYLTEC project

Figure 7 shows analysis of the regions of the aerofoil that require ice protection. The "WIPS normal point" defines the downstream extent of where the whole surface must be heated with no interruptions; as such chambers in this region must be dual use for suction & WIPS. The position where ice protection is no longer required is the "WIPS ultimate point", chambers between this and the "WIPS normal point" can have alternate suction and WIPS chambers. The "Last chamber limit" is the aft most position of the suction chambers to facilitate attachment to the wing box.

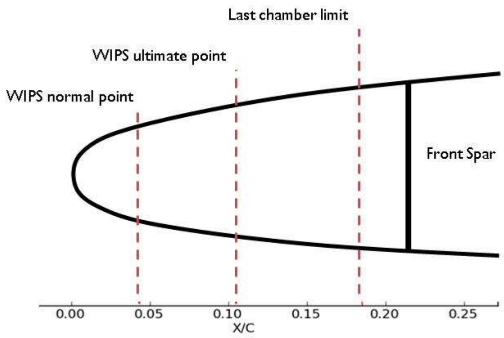

Figure 7: Regions of aerofoil showing WIPS coverage requirements

Figure 8 presents a summary of the chamber layout evolution from Chamber_0 *(used in the analysis previously discussed)* through to the final layout Chamber_210 that was compatible with the manufacturability, WIPS and suction system requirements.

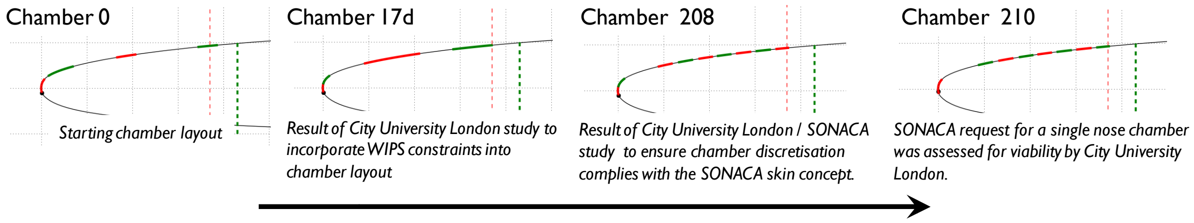

Figure 8: Evolution of suction chamber layout for manufacturability and WIPS requirements

Chamber_17d was the output of a study by City University London to produce a chamber layout that was compatible with the SONACA WIPS requirements and described in[13]. The chamber layout is split into 3 parts each with a specific function. Figure 9 shows a typical suction distribution for chamber layout 17d where it can be seen that the two leading edge chambers control the cross flow modes limiting them to the N-CF constraint of 5 with the aft most chamber effectively controlling the extent of laminarity trading the benefits of increased laminarity (reduced CDv) with increased CD_{pump}. The mid mounted chamber keeps TS modes below the critical level, slightly offloading the aft chamber. The mid mounted chambers become more critical for the C_l=0.63 flow condition.

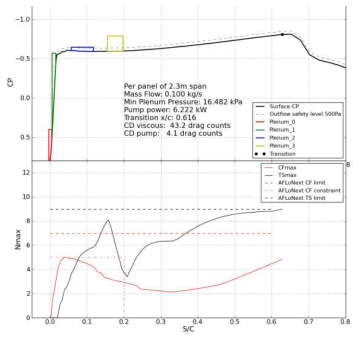

Figure 9: Chamber_17d Suction and N-Factor distribution (C_l=0.55)

Chamber layout 208 resulted from a study between City University London and SONACA (described in ref [14]) , the extents of the suction zones are the same as chamber_17d but the chambers are discretised to conform with the SONACA skin concept.

It has been previously mentioned that the WIPS requires that the leading edge ahead of ≈ 4% chord requires heating without interruptions; unfortunately suction is also required in this area to control the CF waves making it necessary for the suction chambers in this area to be dual use. In an attempt to simplify the HLFC architecture it was decided to combine the two forward chambers of chamber_208 into one larger chamber, creating chamber_210 that will be the subject of the remainder of this paper. Figure 10 presents the chamber layout showing the dual use front chamber and the dedicated WIPS and suction chambers with the corresponding cross section areas. These chamber cross section areas were iterated to get an acceptable compromise between manufacturability and aerodynamic efficiency with regards pressure losses through the spanwise chambers.

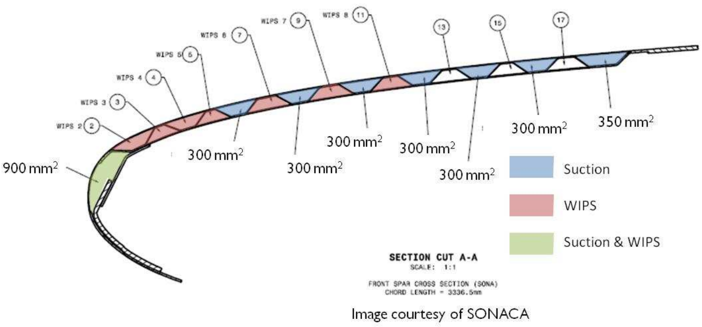

Figure 10: SONACA skin concept showing chambers used for suction & WIPS. (Chamber_210)

Combining the two forward chambers does not come without cost with the suction mass flow and power increasing by 14% relative to the chamber_208 suction layout. Figure 11, shows that higher suction is required largely due to the additional suction in the leading edge chamber necessary to prevent outflow. Additionally the chamber_208 suction distributions TS N-factor envelope is unacceptable from a robustness perspective, with the TS N-factor curve getting perilously close to the critical level at S/C=0.35.

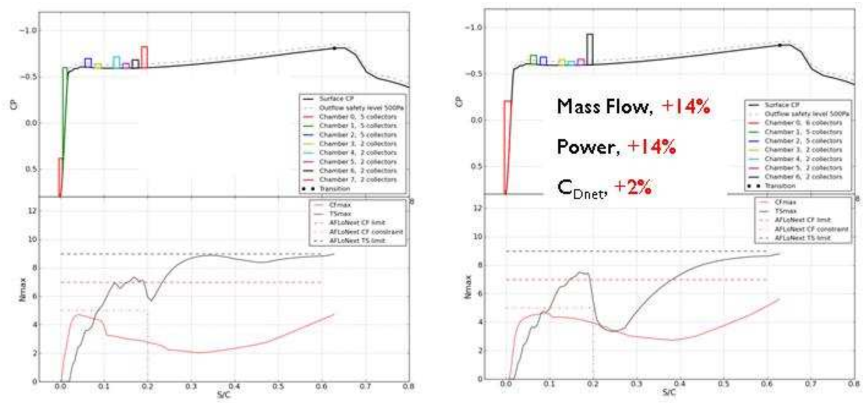

Figure 11 Suction distributions for chamber 208 (left) and 210 (right) for design point C_l=0.55

5 SUCTION DISTRIBUTIONS FOR MULTIPLE DESIGN POINTS

All the previous analysis presented in this paper has concerned suction distributions optimised to minimise CD_{net} for a single design point C_l=0.55. This section will present self adapting suction distributions that can be achieved for each design point (C_l = 0.48, 0.55, 0.68) with a constant metering hole geometry, while variation in suction is achieved with pump rotational speed. In an attempt to achieve this consider a simplified equation for the static pressure levels in the chambers:

$$P_{chamber} - (K_{chamber} * q_{chamber}) = P_{min} - (K_{min} * q_{min}) \qquad \text{Equation (5)}$$

This assumes that the static pressure in the collector is principally driven by the suction chamber with the lowest static pressure "$_{min}$". The term "$(K_{min} * q_{min})$ " is the loss over the metering hole of the suction chamber which we try to be minimal because it is not necessary for any control at this stage. The metering hole losses of all other suction chambers "$_{chamber}$", are however of great importance and will be significantly higher. So assuming that the metering hole loss of the suction chamber with the lowest static pressure is very small (for simplicity) and rearranging the equation, we will have:

$$const = K_{chamber} = \frac{(P_{chamber} - P_{min})}{q_{chamber}} \qquad \text{Equation (6)}$$

Where:
P = static pressure in suction chamber
q = dynamic pressure in suction chamber
K = loss coefficient of metering hole
$_{chamber}$ = given suction chamber
$_{min}$ = suction chamber with lowest static pressure

Equation 6 must hold for any flight condition because K for each suction chamber cannot change (metering hole dimension constant). This also assumes that K is independent of the Reynolds number, which is a reasonable assumption for internal flows through sharp-edged orifices.

Figure 12 shows the result of analysis to obtain a minimum CD_{cost} over the three design points while ensuring the suction system is self-adapting and obeys the imposed design constraints. There are some interesting observations to made here with the C_l=0.63 flow condition having less laminarity indicating that the beneficial effect of increased laminarity is outweighed by the increased pump power. Additionally the C_l=0.48 flow condition has the highest suction & pump power requirements but this is largely due to the requirement of keeping CF N-factor <=5 over the suction panel and the fixed metering hole geometry.

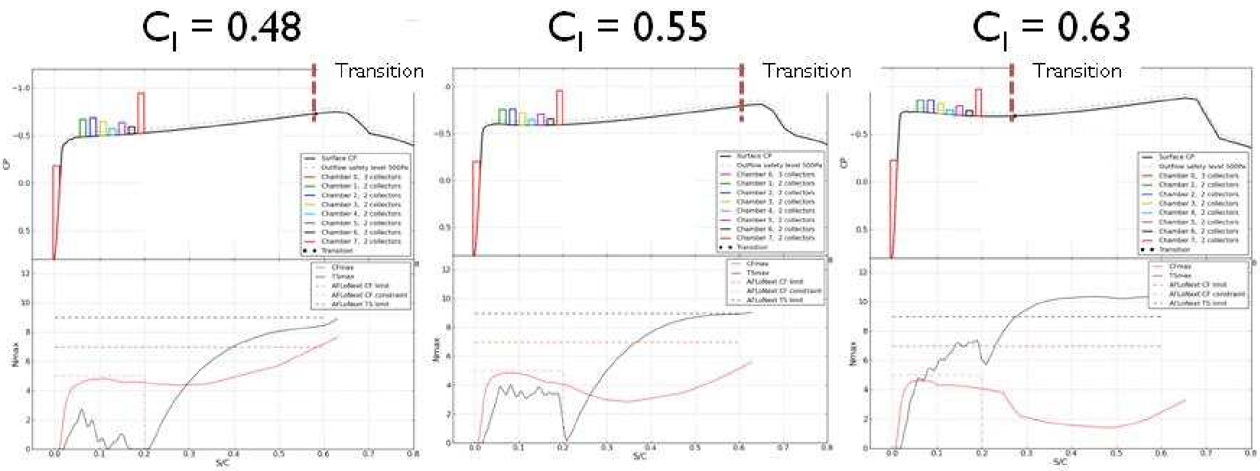

Figure 12: Chamber suction distribution for self adapting suction system for each design point.

6 SENSITIVITY TO SPANWISE CHAMBER PRSSURE VARIATIONS

The analysis in the previous section calculated CD_{net} based on sectional analysis with estimates made of the pressure loss along the spanwise suction chambers. However, no attempt was made to understand how this loss propagates through to a reduction in laminarity. Figure 13 shows the principle of reduced chamber suction levels between metering holes / collector ducts.

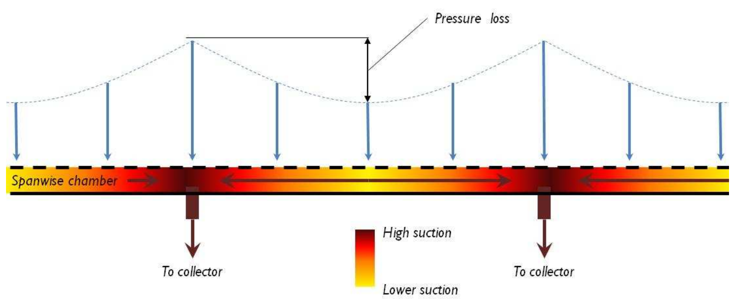

Figure 13 Effect of pressure losses in spanwise chambers on spanwise suction distribution

Figure 14 continues to show the sensitivity of the suction distribution in Figure 12 to increments in suction levels to CD_{cost}. It can be seen that CD_{cost} increases by 1 drag count for every 500Pa increase in chamber suction. In general, increased suction above the levels shown in Figure 12 does not increase laminarity (except for C_l=0.63) but just increases CD_{pump}.

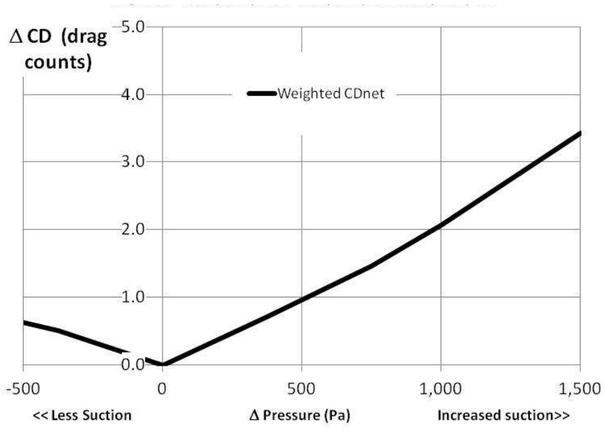

Figure 14 Sensitivity of chamber suction rates on CD_{cost}

7 SUMMARY AND OUTLOOK

This paper has presented an overview of work undertaken by Airbus Group Innovations as part of AFloNext WP1.2 and includes the design of a suitable aerofoil pressure distribution philosophy and self adapting suction distribution while obeying constraints imposed by a particular suction skin concept and ice protection system.

The overall drag benefit from HLFC was reduced as increased realism was introduced into the HLFC systems. The added realism came in the following areas:

- Manufacturability constraints of the skin concept affecting chamber positioning and limitations of chamber cross sectional area tended to increase internal pressure losses of the HLFC ducting leading to increased pump power requirements.
- Incorporation of pneumatic WIPS compromised the leading edge suction chambers into a single chamber, thereby increasing suction rates to control CF modes.
- Allowing a self adapting suction system with fixed metering holes means that each design point is sub-optimal aerodynamically but allows for a relatively simple HLFC architecture.

It has been shown that the spanwise transition variation is relatively robust to changes in suction across the span due to pressure losses along the chambers.

The chamber positioning, chamber cross section area, suction rates and ducting continues to develop within the AFloNext project in response to manufacturability of the skin concept and segregation requirements.

8 ACKNOWLEDGMENTS

AFloNext receives funding from the European Community's Seventh Framework Programme FP7/2007-2013, under grant agreement n° 604013.

REFERENCES

1 Lock R.C, *"An equivalence law relating three- and two-dimensional pressure distributions"* NPL Aero Report no 1028, July 1962
2 Wong P.W.C, Atkin C.J, *"A User's Guide to the transonic aerofoil program CVGK v11"* October 2012
3 Atkin C.J, Gowree E.R, "Recent developments to the viscous Garabedian and Korn method" ICAS 2012.
4 Ashill P.R, Wood R.F, Weeks D.J *"An improved, semi-inverse version of the viscous Garabedian and Korn method (VGK)"* RAE TR 87002, January 1987.
5 Atkin C.J, *"User Guide for CALLISTO (version 3.7)"* June 2013
6 Atkin C.J, *"User Guide for BL2D v3.4"* June 2013
7 Atkin C.J, *"User Guide for CoDS v5.5"* June 2013
8 Atkin C.J, *"HYLTEC TR-81 3D analysis of A310 wing HLFC retrofit & design-for-retrofit performance". HYLTEC TR-81 200#*
9 Miller DS, *"Internal Flow Systems", Ivor Solution ltd, 2012*
10 Idelchik IE, "Handbook of Hydraulic Resistance", Begell House Inc.
11 Atkin C.J, *"Review of porous panel over-suction criteria"* HLYTEC TR-22, June 2001
12 Atkin C.J, *"A new approach to designing the layout of HLFC chambers"*, HLYTEC TR-23, March 2001.
13 Alderman J.E, Atkin C.J, Hui C-Y, *"WP2.1 simplified HLFC wing Deliverable D121.2 Final wing aero shape, initial suction distribution & chamber layout" AFloNext deliverable report April 2014.*
14 Alderman J.E, M Meyer, Atkin C.J, *"Final suction distribution Deliverable D121.7" AFloNext deliverable report October 2014.*
15 Debaisieux S, Overbergh C, Quets S, *"Manufacturing process for a grooved structure and structure obtained by this process" Patent US 20030136815 A1 SONACA S.A*